Res Chem Intermed (2013) 39:1049–1068
DOI 10.1007/s11164-012-0666-y

Synthesis and evaluation of some quinoline Schiff bases as a corrosion inhibitor for mild steel in 1 N HCl

Bhupendra M. Mistry · Smita Jauhari

Received: 10 February 2012 / Accepted: 26 May 2012 / Published online: 3 July 2012

Abstract *N*-((2-chloroquinolin-3-yl)methylene)aniline (**CQM**) and *N*-((2-chloroquinolin-3-yl)methylene)-5-methylthiazol-2-amine (**CQMA**) were synthesized. The effect of **CQM** and **CQMA** have been investigated against mild steel (MS) in 1 N HCl solutions using conventional weight loss, potentiodynamic polarization, linear polarization, electrochemical impedance spectroscopy, UV–Vis spectroscopy and scanning electron microscopic studies. The losses in the weights of MS samples have proved that both **CQM** and **CQMA** are efficient inhibitors. The mixed mode of inhibition was confirmed by electrochemical polarizations. The adsorptions of these inhibitors are found to follow the Langmuir adsorption isotherm. **CQM** and **CQMA** adsorbs on the MS sample by chemisorptions.

Keywords Corrosion inhibitor · EIS · Mild steel · Polarization · SEM · Weight loss

Introduction

There is a continuing effort to find a corrosion inhibitor that exhibits a greater effect with a smaller quantity in the corrosion medium. This is a challenging problem in the steel industry because corrosion over mild steel (MS) surfaces affects long term industrial projects [1–3]. Addition of inhibitor remains the necessary procedure to secure the metal against acid attack in chemical cleaning and pickling to remove mild scales (oxide scale) from the metallic surface. Organic inhibitors are used to protect the metal from corrosion by forming a barrier film on the metal surface. The addition of corrosion inhibitors effectively secures the metal against an acid attack. Inhibitors are used in these processes to control metal dissolution [4–6] and, during

B. M. Mistry · S. Jauhari (✉)
Applied Chemistry Department, S V National Institute of Technology, Surat 395007, Gujarat, India
e-mail: sj.meenu007@gmail.com

the past decade, many organic inhibitors have been studied in different media [7–10]. Their effectiveness is related to the chemical composition, their molecular structure, and their affinities to get adsorbed on the metal surface. The mechanism of their action can be different, depending on the metal, the medium, and the structure of the inhibitor. One possible mechanism is the adsorption of the inhibitor, which blocks the metal surface, and thus does not permit the corrosion process to take place. Organic compounds containing electronegative functional groups and π-electrons in conjugated double or triple bonds generally exhibit good inhibitive properties by supplying electrons via π orbitals. Specific interaction between functional groups containing heteroatoms like N, O, and S having free electron pairs and the metal surface play an important role in inhibition. When both of these features combine, increased inhibition can be observed [11–15].

Schiff base compounds are the condensation products of an amine and a ketone/aldehyde. Recent publications show increased interest in these compounds as corrosion inhibitors especially in acidic environments for protection of various metals like steel, aluminium and copper [16–20]. The greatest advantage of many Schiff base compounds is that they can be conveniently and easily synthesized from relatively cheap materials. Some Schiff bases have been reported earlier as corrosion inhibitors for steel. These compounds, in general are adsorbed on the metal surface blocking the active corrosion sites. A recently reported research revealed that the inhibition efficiency of Schiff's bases are much higher than that of corresponding aldehyde and amines due to the presence of a >C=N– group in the molecules [21]. The planarity (π) and lone pairs of electrons present on N atoms are the important structural features that determine the adsorption of these molecules on the metal surface.

The present work reports the use of a new quinoline derivatives, the *N*-((2-chloroquinolin-3-yl)methylene)aniline (**CQM**) and *N*-((2-chloroquinolin-3-yl)methylene)-5-methylthiazol-2-amine (**CQMA**) (Figs. 1, 2) and investigated their inhibition action on corrosion of MS in 1 N HCl solutions. Corrosion behaviours

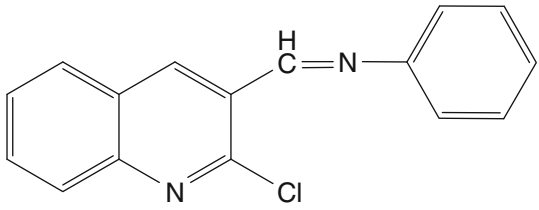

Fig. 1 Molecular *structure* of **CQM**

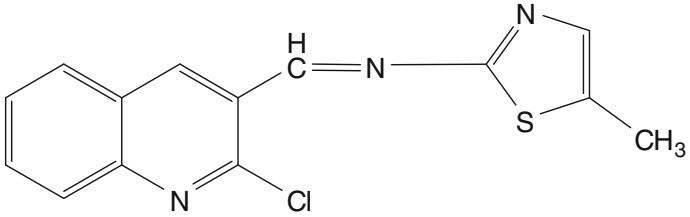

Fig. 2 Molecular *structure* of **CQMA**

of MS in 1 N HCl media in the absence and presence of both the inhibitors have been studied by weight loss (WL) method, potentiodynamic polarization, linear polarization and electrochemical impedance spectroscopy (EIS).

Experimental

Preparation of inhibitor compounds

The compound **CQM** was synthesized by stirring the mixture of 2-chloro-quinoline-3-carbaldehyde (0.005 mol) and aniline (0.005 mol) in ethanol with catalytic amount of sulfuric acid and heated to reflux for 6–7 h. After completion of the reaction (thin layer chromatography), the reaction mixture was poured onto crushed ice; the solid mass thus separated out was filtered, washed with water and dried to give the desired Schiff base compound (**CQM**). Similar procedure was followed for **CQMA**, where the 2-chloro-quinoline-3-carbaldehyde was reacted with 2-amino 5-methyl thiazole [22–24].

*N-((2-chloroquinolin-3-yl)methylene)aniline (**CQM**)*

IR (KBr, cm^{-1}): 1656, 1589, 1531, 760. ^{1}H NMR (400 MHz, DMSO-d_6) δ 7.20–7.35 (m, 5H, Ar–H), 7.52 (m, $J = 1.6$ Hz, 1H, C-1 proton of quinoline), 7.64 (dt, $J = 7.5$, 1.7 Hz, 1H, C-6 proton of quinoline), 7.77–7.80 (m, 2H, C-2 and C-10 proton of quinoline), 7.94 (dd, $J = 8.0$, 1.5 Hz, 1H, C-3 proton of quinoline). 8.91 (s, 1H, –CH=N–). Anal. calcd. for $C_{16}H_{11}ClN_2$: C, 72.05; H, 4.16; N, 10.50 %; found: C, 72.79; H, 4.58; N, 10.89 %.

*N-((2-chloroquinolin-3-yl)methylene)-5-methylthiazol-2-amine (**CQMA**)*

IR (KBr, cm^{-1}): 1670, 1539, 762, 650. ^{1}H NMR (400 MHz, DMSO-d_6) δ 2.41 (s, 3H, Ar-CH_3 at thiazole ring), 7.21 (d, 1H, Ar–H at thiazole ring), 7.52 (m, $J = 1.7$ Hz, 1H, C-1 proton of quinoline), 7.69 (dt, $J = 7.7$, 1.5 Hz, 1H, C-6 proton of quinoline), 7.75–7.83 (m, 2H, C-2 and C-10 proton of quinoline), 7.93 (dd, $J = 8.0$, 1.6 Hz, 1H, C-3 proton of quinoline), 8.76 (s, 1H, –CH=N–). Anal. calcd. for $C_{14}H_{10}ClN_3S$: C, 58.43; H, 3.50; N, 12.32 %; found: C, 58.74; H, 3.70; N, 12.64 %.

Materials

MS specimens obtained from the Metal Samples Company were used as the working electrodes (WEs) throughout the study. The composition of the MS was: 0.09 % P, 0.37 % Si, 0.01 % Al, 0.05 % Mn, 0.19 % C, 0.06 % S and the remainder Fe. The samples of 1×1 cm^2 area were ground with different grades of silicon carbide abrasive papers, i.e. grade 120, 320, 400, 800, 1000, and 2000 to get bright mirror finish followed by rinsed with a large amount of water. Then they were degreased with AR grade ethanol and acetone and dried at room temperature, and

then stored in desiccators before use. The acid solutions were made from analytical grade 37 % HCl by diluting with double-distilled water.

UV–Vis spectral studies

The corrosion products formed on MS surface during polarization was removed by scrapping and was used for recording UV spectra. This study reveals the possibility of the adsorption on the inhibitor on the MS surface. UV was recorded on a Cary 50 Conc spectrophotometer.

Scanning electron microscopy

The surface morphology of the MS specimens immersed in 1 N HCl in presence and absence of the **CQM** and **CQMA** were studied by using scanning electron microscopy (SEM). The immersion time of the electrodes for the SEM analysis was 12 h. immediately after the corrosion tests, the samples were subjected to SEM studies to know the surface morphology. SEM Jeol JSM-5610LV was used for the experiments.

Methods

Potentiodynamic polarization measurements

Polarizations and impedance measurements were carried out using the instrument Electrochemical analyzer model 608 C (USA). Electrochemical experiments were performed in a conventional three electrodes electrochemical cell with a WE of the MS, a pure platinum counter electrode and saturated calomel electrode as a reference electrode. The open circuit potential was recorded after 30 min immersion of WE in the test solution, and then the impedance measurement and the potentiodynamic test. The AC impedance measurements are shown as Nyquist plots and the polarization data as Tafel plots. Polarization resistance measurements were first carried out with a scan rate of 0.01 V/s at −10 to +10 mV versus corrosion potential (E_{corr}) of the WE. The MS electrodes were immersed for 4 h in the test solutions for the impedance measurements which were carried out at the E_{corr}.

Electrochemical impedance spectroscopy (EIS)

EIS was employed as a sophisticated and established laboratory technique with the relevant software to determine the important parameters like the charge transfer (corrosion) resistance (R_t) rate and double layer capacitance (C_{dl}) [25–29]. Using Electrochemical analyzer model 608 C (USA) the AC impedance measurements were carried out in the range of 0.1–1,000 Hz. The AC signal was 5 mV peak-to-peak, with 12 data points per decade. The same cell and system as in the polarization method was used. The double layer capacitance (C_{dl}) and the charge transfer resistance (R_t) were calculated from Nyquist plots.

WL method

The WL of MS in 1 N HCl solutions in the presence and absence of various concentrations of the inhibitors **CQM** and **CQMA** were determined after 4 h period of immersion using glass hooks and rods. The mass of the specimens before and after immersion was determined using an analytical balance of 0.01 mg accuracy. The tests were performed at various temperatures (with ±1 °C accuracy) controlled by using a thermostated water bath. All the aggressive acid solutions were open to air. From the WL data, the percentage inhibition efficiency (E_w%) was calculated at different concentrations at 25–35 °C.

Results and discussion

Potentiodynamic (Tafel) polarization measurements

The numerical values of the variation of corrosion potential (E_{corr}), the corrosion current density (I_{corr}), the anodic and cathodic Tafel slopes (b_a and b_c) with the concentrations of **CQM** and **CQMA** are given in Table 1. These values were calculated from the Tafel fit routine provided by CH Electrochemical analyzer model 608 C (USA). The values of inhibition efficiency (E_I%) were calculated using the following equation:

$$E_I\% = 100 \times \frac{I_{corr} - I_{corr(inh)}}{I_{corr}} \quad (1)$$

where I_{corr} and $I_{corr(inh)}$ represents the values of corrosion current densities without and with the additives, respectively and were determined by extrapolation of the

Table 1 Tafel polarization parameter values for the corrosion of MS in 1 N HCl solution containing different concentrations of **CQM** and **CQMA**

Inhibitor	IC (mg kg^{-1})	$-E_{corr}$ (V)	k[a] (mV per decade)		I_{corr} (mA cm^{-2})	R_p (Ω cm^2)	E_I%	E_{RP}%
			b_a	b_c				
CQM	1 N HCl	0.508	145	135	4.0800	7	–	–
	5	0.440	74	91	0.3279	57	91.96	87.71
	10	0.450	79	93	0.2740	76	93.28	90.78
	15	0.453	90	95	0.1983	103	95.13	93.20
	20	0.460	93	102	0.1557	124	96.18	94.35
	25	0.461	101	112	0.1410	148	96.54	95.27
CQMA	1 N HCl	0.508	145	135	4.0800	7	–	–
	5	0.456	79	143	0.1250	178	96.93	96.06
	10	0.463	82	134	0.0914	243	97.75	97.11
	15	0.468	91	132	0.0738	317	98.19	97.79
	20	0.475	123	154	0.0598	498	98.53	98.59
	25	0.499	138	143	0.0342	891	99.19	99.21

[a] Tafel constant

cathodic and anodic Tafel lines to the corrosion potential E_{corr}. It was found from Table 1 that the values of E_I% were increased with increase in the concentration of both the additives. This study has indicated that by increasing the inhibitors concentration, the corrosion current density was decreased and the corrosion potential (E_{corr}) was shifted slightly to more positive values. Also, the inhibition efficiency E_I% was increased. At the highest concentration of 25 ppm, the values of E_I% were 96.54 and 99.19 % for **CQM** and **CQMA** respectively.

The inhibiting properties of the **CQM** and **CQMA** have also been evaluated by determining the polarization resistance R_p (Ω cm^2). The corresponding polarization resistance (R_p) values for MS in 1 N HCl solutions in the absence and presence of different concentrations of the additives are given in Table 1. The values of inhibition efficiency (E_{RP}%) were calculated as follows:

$$E_{RP}\% = 100 \times \frac{R_{p(inh)} - R_p}{R_{p(inh)}} \quad (2)$$

where R_p and $R_{p(inh)}$ are the polarization resistances in the absence and presence of the additives, respectively.

Both Fig. 3a and b revealed that an increase in the inhibitor concentration leads to block more anodic sites which were responsible for the metal dissolution. Adsorption of organic inhibitor molecules onto a metal surface retarding the metal dissolution and as a consequence hydrogen evolution by blocking the active sites on the MS or even can screen the covered part of the electrode and therefore protect it from the action of the corrosion medium [30, 31]. The variation of b_c values with altering in type and concentration of inhibitors indicated that there was an influence of the compounds added on the kinetics of hydrogen evolution. Also, the shift in the anodic Tafel slope (b_a) may be due to the adsorption of chloride ions/or inhibitor molecules adsorbed onto the steel surface [32]. The presence of **CQM** and **CQMA** did not prominently shift the corrosion potential, which confirmed that both the studied quinoline derivatives have acted as mixed-type inhibitors. Furthermore, in the presence of either compound, the slight change of both b_c and b_a has indicated that the corrosion mechanism of MS does not change. These results proved that these inhibitors have acted by simple blocking of the available surface area [33]. In other words, these inhibitors have decreased the active surface area for the acid corrosion attack without affecting the mechanism of corrosion and only caused inactivation of a part of the metal surface with respect to the corrosive medium R_p.

The R_p values of MS in 1 N HCl solution in the absence and presence of different concentrations of the tested additives are also given in Table 1. The results obtained in Table 1 inferred that the R_p values were gradually increased with increase in the concentration of the additives. The values of inhibition efficiency (E_{RP}%) of **CQM** and **CQMA** were in good agreement with those of E_I% obtained by the electrochemical methods.

Electrochemical impedance spectroscopy (EIS)

EIS was employed in order to investigate the surface layer created by inhibitors. The effect of inhibitor concentration on the impedance behaviour of MS in 1 N HCl

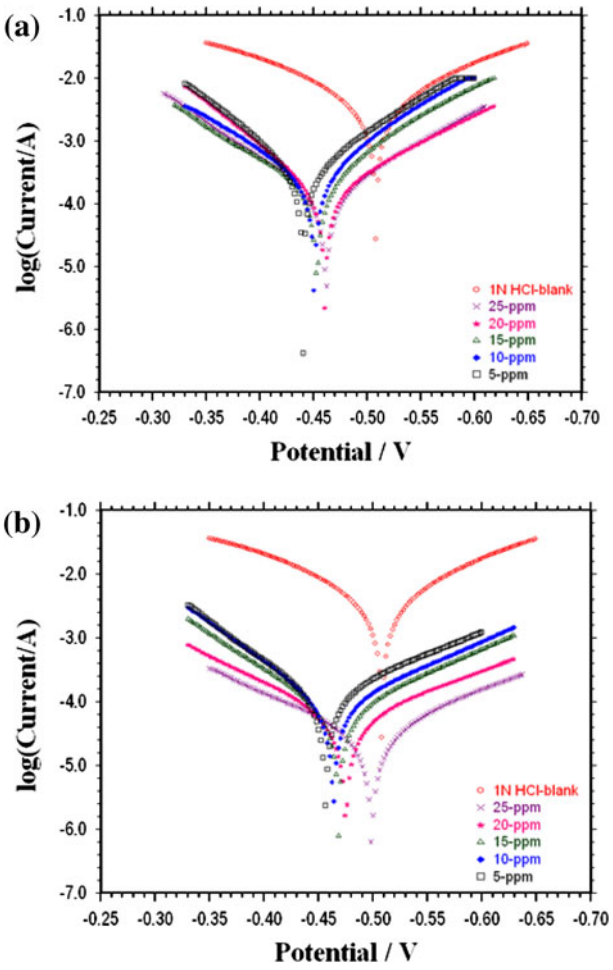

Fig. 3 Tafel *plots* showing the effect due to **a CQM** and **b CQMA** on the corrosion of MS in 1 N HCl solution

solutions containing different concentrations of **CQM** and **CQMA** are presented in Fig. 3 at 25 °C.

The values of inhibition efficiency ($E_R\%$) were calculated by following the equation:

$$E_R\% = 100 \times \frac{R_{t(inh)} - R_t}{R_{t(inh)}} \tag{3}$$

where R_t and $R_{t(inh)}$ are the charge transfer resistances ($\Omega\,cm^2$) values in the absence and presence of the additives, respectively. Further, To get the values of double layer capacitance (C_{dl}), the values of frequency (f_{max}) at which the maximum

imaginary component of the impedance $-Z_{\mathrm{im(max)}}$ were found, and were used in the following equation with corresponding R_t values:

$$C_{\mathrm{dl}} = \frac{1}{2\pi f_{\max} R_t} \tag{4}$$

Nyquist plots in Fig. 4a and b contained depressed semi-circles with the centre under the real axis, whose size increased with the increase in the concentration of additives, which confirmed that the charge transfer processes were mainly controlling the corrosion of MS. An isolated Nyquist plot for MS in the blank system is shown in Fig. 4c, and the value of real impedance (Z') was minimum only 12 Ω cm^2 which confirmed that there was least charge transfer resistance (R_t) of the acid corrosion reactions. In presence of both the inhibitors, comparing with blank system, the shape was maintained throughout all tested concentrations, indicating that there was almost no change in the corrosion mechanism due to the inhibitor addition. There was a gradual increase in the diameter of each of the semicircles of the Nyquist plots when the concentrations were raised from 5 to 25 ppm in Fig. 4a and b. This gradual increase of the diameters corroborated that the R_t values were increased up to the highest concentration of 25 ppm.

These capacitive loops are not perfect semicircles which can be attributed to the frequency dispersion effect as a result of the roughness and inhomogeneities of the MS electrode surface [34]. Furthermore, the diameter of the capacitive loop in

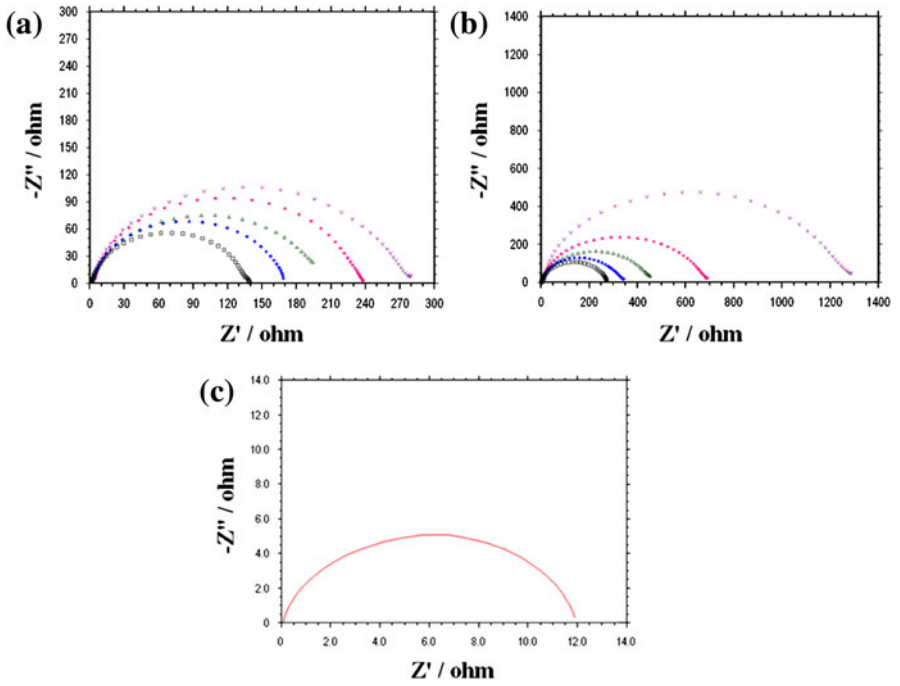

Fig. 4 Showing the effect of **a CQM** and **b CQMA** on the corrosion of MS in 1 N HCl solution (*times* 25 mg kg^{-1}, *stars* 20 mg kg^{-1}, *triangles* 15 mg kg^{-1}, *diamonds* 10 mg kg^{-1} and *squares* 5 mg kg^{-1}) **c** Nyquist *plot* in 1 N HCl blank system

the presence of inhibitor was bigger than that in the absence of inhibitor (blank solution) and was increased with the increase in the inhibitor concentration, which confirmed that the impedance of inhibited surface of the MS increased with the inhibitor concentration.

For corrosion reactions which are strictly charge transfer controlled, impedance behaviour can be explained with the help of a simple and commonly used equivalent circuit which composed of a double layer capacitance, R_t and R_s. The resistor R_s is in series to the double layer capacitance and R_t while double layer capacitance is parallel to R_t. The double layer capacity is in parallel with the impedance due to the charge transfer reaction. This type of circuit has been used previously to model the iron–acid interface [35, 36]. The constant phase element, CPE, is introduced in the circuit instead of a pure double layer capacitance to give more accurate fit as shown in the Fig. 5 [37].

Table 2 summarizes the values of R_t and C_{dl}. There was a gradual decrease in the value of C_{dl} with an increase in the concentration of both **CQM** and **CQMA**. The double layer between the charged metal surface and the solution has been considered as an electrical capacitor. The adsorption of the **CQM** and **CQMA** on the MS electrode leads to a decrease of its electrical capacity because they might have displaced the water molecules and other ions originally adsorbed on the MS surface [38, 39]. The decrease of this capacity with the increase in the concentrations of **CQM** and **CQMA** was associated with the formation of a protective layer on the MS electrode surface. The inhibition efficiency $E_R\%$ was found to increase with an increase in the concentrations of **CQM** and **CQMA**. Decreasing the double layer capacitance, C_{dl}, was resulted from the decrease in local dielectric constant due to the increase of electrical double layer thickness. This has proved that the role of inhibitor molecules was preceded by the adsorption at the metal–solution interface. Therefore, the **CQM** and **CQMA** molecules function by adsorption at the metal–solution interface. Another evidence for the effective adsorption of **CQM** and **CQMA** on the steel surface could be given from the observation that the maximum frequency (f_{max}) of the capacitive loop of the uninhibited solution was decreased with increasing the inhibitor concentration.

The results obtained have proved that the corrosion rate of MS was significantly decreased due to the adsorption mechanism affecting both the anodic and cathodic processes. The nature of interaction between the MS surface and the inhibitors could be established by isotherm which has described the adsorption behaviour of the inhibitor on the MS surface.

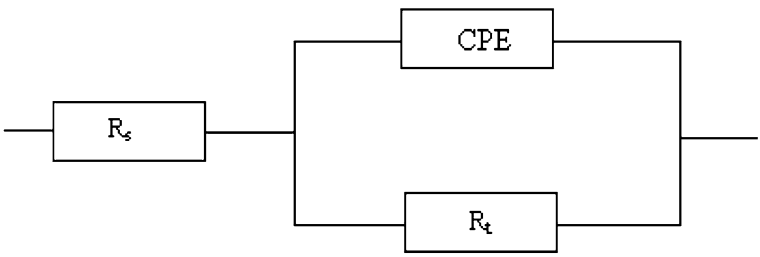

Fig. 5 Equivalent circuit used to fit the EIS data

Table 2 Electrochemical impedance parameters for MS in 1 N HCl solution in the presence of different concentrations of **CQM** and **CQMA**

Inhibitor	IC (mg kg^{-1})	R_t (Ω cm^2)	C_{dl} (μF cm^2)	E (%)
CQM	1 N HCl	12	163	–
	5	140	141	91.42
	10	170	116	92.94
	15	210	78	94.28
	20	240	68	95.00
	25	280	48	95.71
CQMA	1 N HCl	12	163	–
	5	270	73	95.55
	10	350	56	96.57
	15	470	35	97.44
	20	700	23	98.28
	25	1300	10	99.07

IC inhibitor concentration

WL measurements

The corrosion of MS in 1 N HCl solutions in the absence and presence of various concentrations (5–25 ppm) of **CQM** and **CQMA** has been studied by the WL experiments. The corrosion rate (W_{corr}) and the values of inhibition efficiency (E_w%) were calculated according to the following equation:

$$E_w\% = 100 \times \frac{W_0 - W_{corr}}{W_0} \tag{5}$$

where W_{corr} and W_0 are the corrosion rates of MS with and without the additives, respectively.

The values of inhibition efficiency (E_w%) and corrosion rate (W) were obtained from WL measurements with the addition of various concentrations of **CQM** and **CQMA** after 4 h of immersion in 1 N HCl solutions. The results summarized Table 3 inferred that both the quinoline derivatives **CQM** and **CQMA** have inhibited the corrosion of MS in 1 N HCl solutions at all concentrations. The inhibition efficiency (E_w%) was increased with an increase in the concentration of the additives which has confirmed that the number of molecules adsorbed were increased over the MS surface, blocking the active sites of acid attack and, thereby, protecting the MS from corrosion. At 25 ppm of each additives studied, the E_w% attained was maximum 90.13 % for **CQM** and 95.06 % for C**QMA**, which has also confirmed that both the additives were very effective as inhibitors for MS in 1 N HCl solutions.

Effect of temperature

To study the effect of temperature on the inhibition efficiencies of **CQM** and **CQMA**, WL measurements were carried out in the temperature range 25–45 °C in absence and presence of inhibitors at optimum concentrations for 3 h of immersion. The corresponding data are shown in Table 5. The apparent activation energies for the steel dissolution process can be evaluated from the following relationship:

$$W^o = K^o \exp\left(-\frac{E_a^o}{R \cdot T}\right) \quad (6)$$

$$W = K \exp\left(-\frac{E_a}{R \cdot T}\right) \quad (7)$$

where K^o and K are the rate constants, E_a and E_a^o are the activation energies for the corrosion in the presence and absence of the inhibitor, respectively. T is the absolute temperature in Kelvin and R is the universal gas constant. The logarithm of the corrosion rate of steel W_{corr} can be represented as straight-lines function of $1/T$ (Arrhenius equation) in Fig. 6.

Table 3 Inhibition efficiency of MS in 1 N HCl solution in the presence and absence of different concentrations of **CQM** and **CQMA** (WL method)

Inhibitor	IC (mg kg^{-1})	W (μg cm^{-2} h^{-1})	E_w%
CQM	1 N HCl	17.63	–
	5	2.88	83.66
	10	2.73	84.51
	15	2.38	86.50
	20	2.07	88.25
	25	1.74	90.13
CQMA	1 N HCl	17.63	–
	5	2.08	88.20
	10	1.69	90.41
	15	1.41	92.00
	20	1.15	93.47
	25	0.87	95.06

IC inhibitor concentration

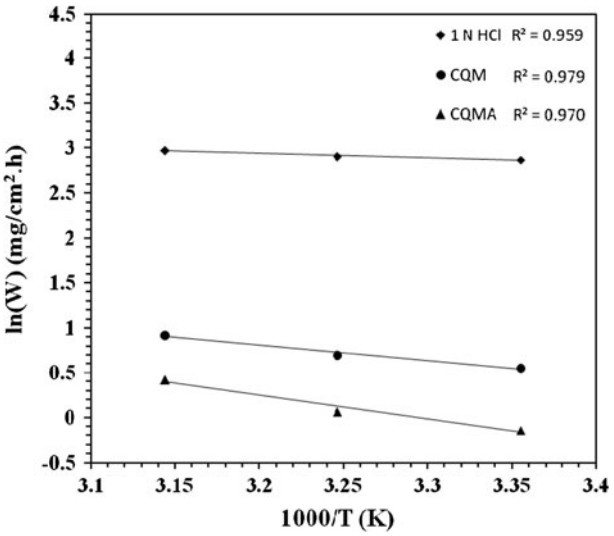

Fig. 6 Arrhenius plots of MS in 1 N HCl in absence and presence of 25 ppm of **CQM** and **CQMA**

The temperature effect depicts the absorbance of **CQM** and **CQMA** on the MS surface at all temperatures. It was found that there is change in the corrosion rates in absence and presence of inhibitors in 1 N HCl solutions. Corrosion of metal in acidic media is accompanied with evolution of H_2 gas, as there is increase in the corrosion rate with increase in temperature due to higher dissolution rate of the metal. Table 5 shows that the corrosion rate with respect to temperature in absence and presence of 1 N HCl solutions. The values of inhibition efficiency for **CQMA** decreased from 95.06 at 25 °C to 92.21 % at 45 °C, similarly, for **CQM** it decreased from 90.13 at 25 °C to 87.17 % 45 °C. Figure 6 shows the logarithm of the corrosion rate of steel which can be represented as a straight-line function of $1/T$, where T is the temperature in Kelvin. All the linear regression coefficients were close to 1, indicating that the MS corrosion in hydrochloric acid can be found out using the kinetic model. The activation energy could be determined from the Arrhenius plots for steel corrosion rate presented in Fig. 6. Equations (6) and (7) can be used to calculate E_a values of the corrosion reaction in the absence and presence of **CQM** and **CQMA** which are $E_a^o = 4.27$ kJ mol^{-1} for blank, $E_a = 14.58$ for **CQM** and $E_a = 22.15$ kJ mol^{-1} for **CQMA**, respectively. The increase in the apparent activation energy may be interpreted as physical adsorption that occurs in the first stage [40]. The increase in activation energy can be stated as to an appreciable decrease in the adsorption of the inhibitor on the MS surface with increase in temperature. Desorption of inhibitor molecule occurs with decreases in adsorption as these two opposite processes are in equilibrium. As desorption increases of inhibitor molecules at higher temperatures, the greater surface area of MS comes in contact with aggressive environment, resulting increased corrosion rates with increase in temperature [41].

Adsorption isotherm

Basic thermodynamic information on the interaction between inhibitor molecules and the metal surface can be provided by the adsorption isotherm. The efficiency of both molecules as a successful corrosion inhibitor mainly depended on their adsorption ability on the MS surface. The adsorption process consisted of the replacement of water molecules at a corroding interface according to following process [42].

$$\mathrm{Org}_{(\mathrm{sol})} + n\mathrm{H_2O}_{(\mathrm{ads})} \rightarrow \mathrm{Org}_{(\mathrm{ads})} + n\mathrm{H_2O}_{(\mathrm{sol})} \tag{8}$$

where $\mathrm{Org}_{(\mathrm{sol})}$ and $\mathrm{Org}_{(\mathrm{ads})}$ are the organic molecules studied in the solutions and adsorbed on the MS surface, respectively, and n is the number of water molecules replaced by the organic molecules.

In order to obtain the isotherm, the surface coverage (θ) values as a function of inhibitor concentration must be obtained. The surface coverage (θ) at different concentrations of **CQM** and **CQMA** in 1 N HCl solution was calculated from the corrosion rates obtained by the WL measurements using the following equation:

$$\theta = \frac{W_0 - W}{W_0} \tag{9}$$

where W_0 and W are the corrosion rates in the absence and presence of the inhibitors, respectively. Then attempts were made to fit the θ values to various isotherms including Langmuir, Temkin and Frumkin. Among all these adsorption isotherms, the Langmuir adsorption isotherms were found to be the best description for the adsorption behaviour of the inhibitors studied.

Langmuir adsorption isotherm can be expressed by the following equation:

$$\frac{C}{\theta} = \frac{1}{K_{\text{ads}}} + C \tag{10}$$

where K_{ads} is the equilibrium constant of the inhibitor adsorption process and C is the inhibitor concentration. Plots of C/θ versus C yielded a straight line, as shown in Fig. 7. In both the cases, the linear regression coefficients (R^2) were almost equal to 1, indicating that the adsorption of **CQM** and **CQMA** obeyed the Langmuir adsorption isotherm. Further, the K_{ads} values were calculated from the intercepts of the straight lines on the C/θ-axis. The constant of adsorption (K_{ads}) has been related to the standard free energy of adsorption, ΔG^0_{ads} with the following equation:

$$\Delta G_{\text{ads}} = -2.303RT \log(55.5K_{\text{ads}}) \tag{11}$$

where K_{ads} is the equilibrium constant of adsorption, R is the gas constant, T is absolute temperature, and the value 55.5 is the molar concentration of water solution in mol L^{-1}.

The K_{ads} values obtained from the Langmuir adsorption isotherm are listed in Table 4, together with the values of the Gibbs free energy of adsorption ΔG^0_{ads}. The high values of K_{ads} for **CQM** and **CQMA** have proved that there was stronger

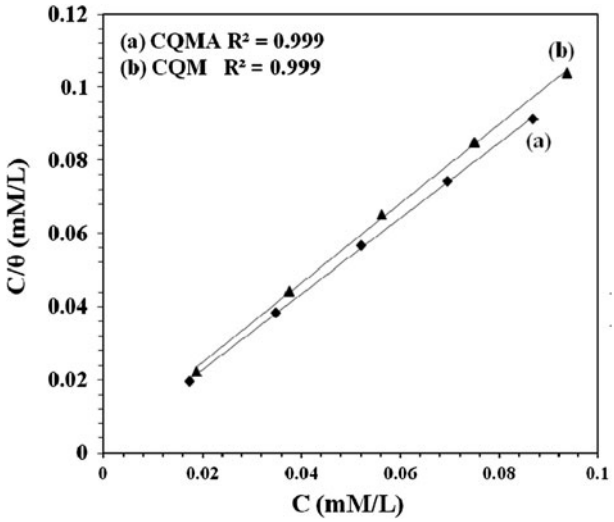

Fig. 7 Langmuir isotherm adsorption of **CQM** and **CQMA** on MS in 1 N HCl at room temperature

Table 4 Thermodynamic parameters for adsorption of **CQM** and **CQMA** on MS in 1 N HCl solution

Inhibitor	ΔG^0_{ads} $(kJ\ mol^{-1})^a$	ΔH^0_{ads} $(kJ\ mol^{-1})^a$	ΔS^0_{ads} $(J\ K^{-1}\ mol^{-1})^a$
CQM	−41.66	−11.62	100.8
CQMA	−42.53	−19.07	78.72

[a] Values are calculated at 298 K

adsorption on the MS surface in 1 N HCl solutions. The addition of inhibitors caused negative values of ΔG^0_{ads} which have confirmed that the inhibitors **CQM** and **CQMA** were adsorbed spontaneously. It has been generally accepted that, for ΔG^0_{ads} values up to −20 kJ mol^{-1}, the type of adsorption was regarded for physisorption because the inhibitors acted due to the electrostatic interactions between the charged molecules and the charged metal surface, while the values around −40 kJ mol^{-1} were considered for as chemisorptions [43–45] which was due to the charge sharing or a transfer from the inhibitor molecules to the metal surface to form a covalent bond. In the present study, the values of ΔG^0_{ads} were −41.66 kJ mol^{-1} for **CQM** and −42.53 kJ mol^{-1} for **CQMA** found at 298 K, the calculated standard free energy of adsorption value is closer to −40 kJ mol^{-1}. Therefore it can be concluded that the adsorption of the **CQM** and **CQMA** on the MS surface is more chemical than physical one. [46].

The effect of temperature on the corrosion of the MS in the absence and presence of the inhibitors in 1 N HCl solutions was studied by using WL method in the temperature range of 25–45 °C and at optimum concentrations. Thermodynamic parameters are important in studying adsorption of organic inhibitors on MS. The heat of adsorption (ΔH) was calculated using the Van't Hoff equation [47]:

$$lnK = \frac{-\Delta H}{RT} + constant \tag{12}$$

Figure 8 shows the straight line between $1/T$ (K^{-1}) versus log ($\theta/1-\theta$). The slope of these straight lines is equal to $-\Delta H_{ads}/2.303R$. The heat of adsorption (ΔH^0_{ads}) could be approximately regarded as the standard adsorption heat (ΔH^0_{ads}) under experimental conditions [48]. Further, the standard entropy of adsorption (ΔS^0_{ads}) was obtained by following the thermodynamic basic equation:

$$\Delta S^0_{ads} = \frac{\Delta H^0_{ads} - \Delta G^0_{ads}}{T} \tag{13}$$

All the calculated thermodynamic parameters are listed in Table 5. The values of thermodynamic parameters for the adsorption of inhibitors could provide valuable information about the mechanism of corrosion inhibition. While an endothermic adsorption process ($\Delta H^0_{ads} > 0$) is attributed unequivocally to chemisorption, an exothermic adsorption process ($\Delta H^0_{ads} < 0$) may involve physisorption, chemisorption or a mixture of both [49]. In an exothermic process, physisorption can be distinguished from chemisorption by considering the absolute value of ΔH^0_{ads}. For physisorption processes, this magnitude is usually lower than 40 kJ mol^{-1} while that for chemisorptions approaches 100 kJ mol^{-1} [50]. In the present work, the

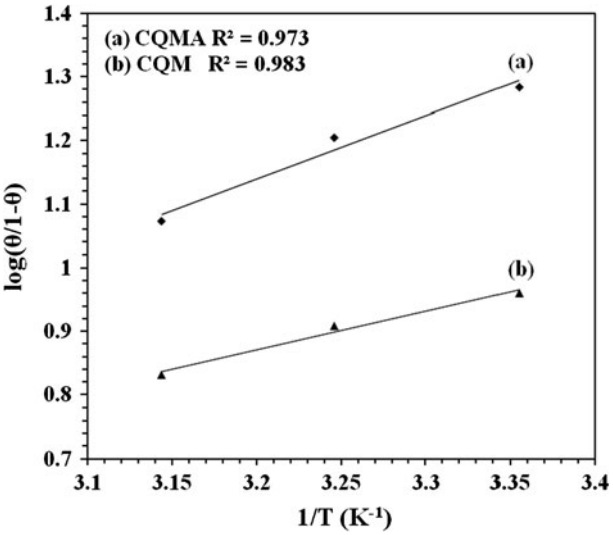

Fig. 8 *Plots* of $1/T\,(K^{-1})$ versus $\log(\theta/1-\theta)$ for adsorption of **CQM** and **CQMA** on the MS in 1 N HCl solution

Table 5 Various corrosion parameters and free energy of adsorption for MS in 1 N HCl containing optimum concentration of **CQM** and **CQMA** at different temperatures

Inhibitor	Temperature (K)	CR (mg cm^{-2} h^{-1})	Surface coverage (θ)	IE (%)	ΔG^0_{ads} ($kJ\,mol^{-1}$)
Blank	298	17.63	–	–	–
	308	18.29	–	–	–
	318	19.65	–	–	–
CQM	298	1.74	0.9013	90.13	−41.66
	308	2.01	0.8901	89.01	−43.08
	318	2.52	0.8717	87.17	−44.53
CQMA	298	0.87	0.9506	95.06	−42.53
	308	1.07	0.9414	94.14	−43.99
	318	1.53	0.9221	92.21	−45.47

CR corrosion rate

negative sign of ΔH^0_{ads} has shown that the adsorption of inhibitors used was exothermic. The absolute values of ΔH^0_{ads} for adsorption of **CQM** and **CQMA** are 11.62 and 19.07 kJ mol^{-1}, respectively, which were lower than 40 kJ mol^{-1} and indicate that the possibility of physisorption. Moreover, the positive sign of ΔS^0_{ads} is also related to substitutional process which can be attributed to the increase in the water desorption entropy [51, 52]. It is also interpreted that with the increase of disorders due to the more water molecules desorbed from the metal surface causes an increase in the disorders of the system [53].

UV–Vis spectral studies

UV–Vis adsorption spectra obtained from the corrosive solution of 25 ppm **CQM** and **CQMA** before and after 4 h of MS immersion are shown in Fig. 9. The electronic adsorption spectra of **CQM** and **CQMA** before the MS immersion display two bands for **CQM** and one band for **CQMA** in UV region. The shorter wavelength band with λ_{max} at 281 nm and λ_{max} at 400 nm are ascribed to π–π^* and n–π^* transition for **CQM** and band with λ_{max} at 365 nm is due to n–π^* transition for **CQMA**. After 4 h of MS immersion clear changes are observed in absorbance which depicts the charge transfer

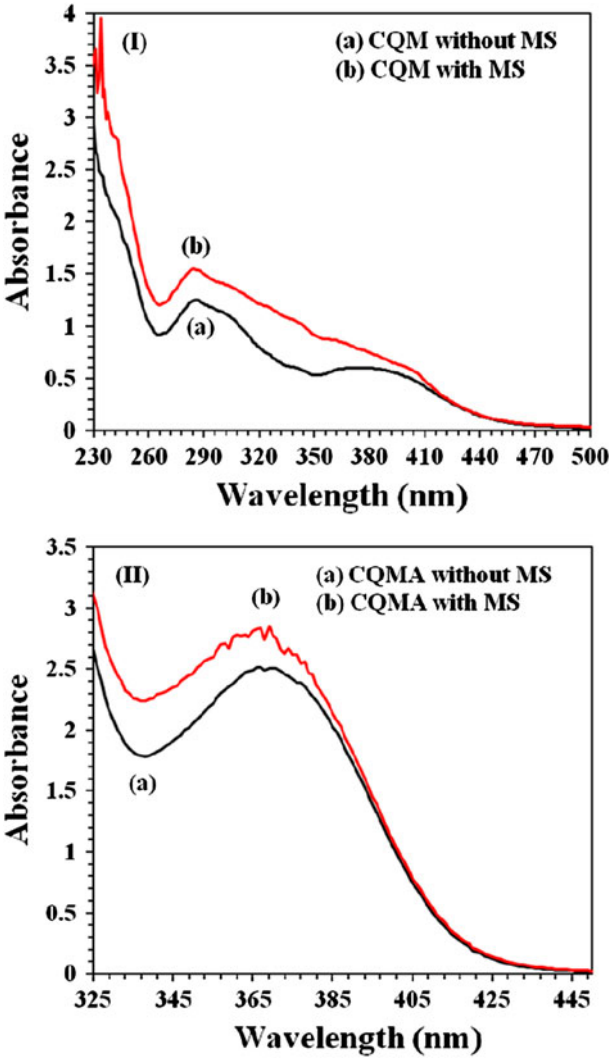

Fig. 9 UV–Vis spectra of the solution containing 25 ppm CQM and CQMA + 1 M HCl before (**a**) and after (**b**) 4 h of MS immersion

process occurring due to possible interaction between the ligand and Fe. These experimental findings give a strong evidence for the possibility of the formation of a complex between Fe^{2+} cation and inhibitor in 1 N HCl solution.

In order to evaluate the conditions of the MS surfaces in contact with 1 N HCl acid solutions, a superficial analysis was carried out. Figure 10a shows the polished MS sample. Figure 10b shows SEM images of the surface of the MS specimens after immersion in 1 N HCl solutions with no additives for duration of 12 h. The surface shown in the Fig. 10b was a result of cracks caused by corrosion attack due to exposure of MS into 1 N HCl solution. Figure 10c and d show images of the surface of the MS specimens immersed for 12 h in 1 N HCl acid solutions containing 25 ppm **CQM** and **CQMA**. As can be seen from Fig. 10c and d, that there was much less damage on the surface of MS with **CQMA** than that compared to **CQM**. This was due to strong adsorption of **CQMA** on the MS surface in 1 N HCl solution. Therefore it could be evidenced from Fig. 10d that the corrosion was strongly inhibited when **CQMA** was present in 1 N HCl solution.

Inhibition mechanism

The mechanism of the action of inhibitors in acid solutions has been studied extensively. It is generally believed that these compounds are adsorbed on the metal

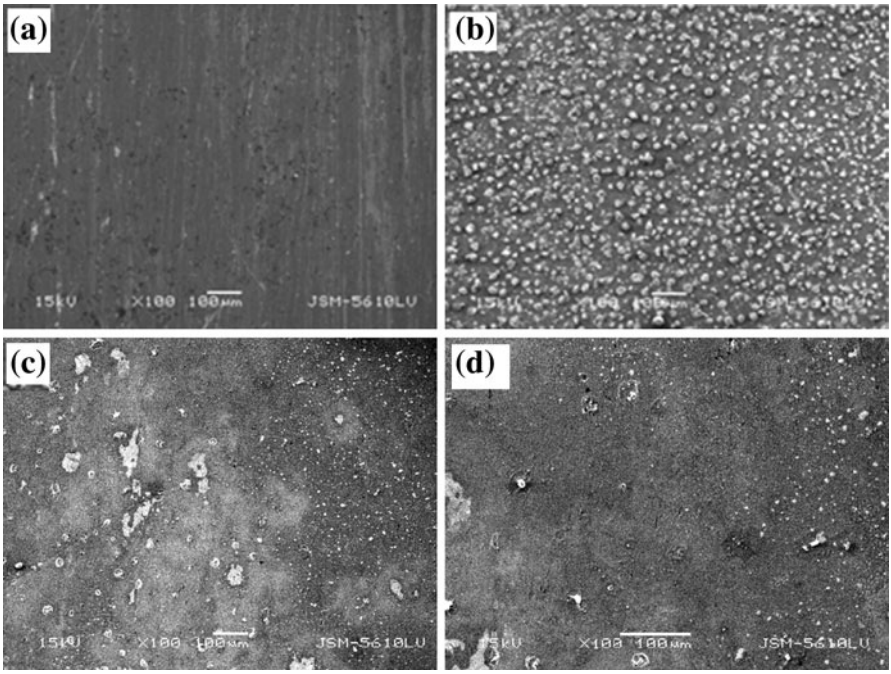

Fig. 10 SEM *micrographs* of MS samples after 12 h immersion period **a** polished surface, **b** after 12 h immersion in 1 N HCl, **c** after 12 h immersion in 1 N HCl + 25 ppm **CQM**, **d** after 12 h immersion in 1 N HCl + 25 ppm **CQMA**

surface and prevent further dissolution of metal through blocking of either the cathodic or anodic reaction or both. Another group of organic inhibitors, which has been the focus of attention in recent years, are those organic compounds capable of forming insoluble complexes, or chelate, with metallic ions present on the surface of metal. The inhibition efficiency of **CQM** and **CQMA** against the corrosion of MS in 1 N HCl solution could be explained on the basis of the number of adsorption sites, their charge density, molecular size, mode of interaction with the MS surface and ability to from the metallic complexes. The possible mechanism of corrosion inhibition of MS in 1 N HCl solution by the compounds under study could be deduced on the basis of adsorption.

In addition to the chemical adsorption, the inhibitor molecules can also be adsorbed on the steel surface via electrostatic interaction between the charged metal surface and the charged inhibitor molecules if it is possible. The anodic dissolution of iron follows the steps given below [54]:

$$Fe + Cl^- \leftrightarrow (FeCl^-)_{ads} \tag{14}$$

$$(FeCl^-)_{ads} \leftrightarrow (FeCl)_{ads} + e^- \tag{15}$$

$$(FeCl)_{ads} \rightarrow (FeCl^+) + e^- \tag{16}$$

$$(FeCl^+) \leftrightarrow Fe^{2+} + Cl^- \tag{17}$$

It is well known that the chloride ions have a small degree of hydration, and due to specific adsorption, they should be first adsorbed on the positively charged metal surface according to reaction (14). The adsorption of chloride ions has created an excess negative charge towards the solution side of metal and favours more adsorption of cations [55]. Then the inhibitor molecules were adsorbed through electrostatic interactions between the negatively charged MS surface and positively charged molecule ($\mathbf{CQM^+}$ and $\mathbf{CQMA^+}$) and formed a protective ($FeCl^-$ $\mathbf{CQM^+}$, $FeCl^-$ $\mathbf{CQMA^+}$)$_{ads}$ layer. In this way, the oxidation reaction of $(FeCl^-)_{ads}$ is shown by reaction steps from (15) to (17) [56, 57]. The cathodic hydrogen evolution reaction may be given as follow:

$$Fe + H^+ \leftrightarrow (FeH^+)_{ads} \tag{18}$$

$$(FeH^+)_{ads} + e^- \rightarrow (FeH)_{ads} \tag{19}$$

$$(FeH)_{ads} + H^+ + e^- \rightarrow Fe + H_2 \tag{20}$$

Analysis of the electrochemical data showed that the inhibiting properties increased with an increase in the concentrations of **CQM** and **CQMA**. The presence of the electron donating groups on the structure increases the electron density on the N atom, resulting into higher inhibition efficiency. Among the two compounds investigated in the present study, **CQMA** was found to give the better performance as a corrosion inhibitor. This could be explained on the basis of the presence of heterocyclic thiazole ring in **CQMA**. Therefore, based on the present experimental findings, firstly the chloride ions of hydrochloric acid get adsorbed on the metal surface, and in steps led to the formation of ferrous ions. Thereafter, the inhibitor

molecules were attracted towards the MS surface and interacted coordinatively with ferrous ion and than adsorbed on the MS surface to protect the corrosion.

Conclusions

(1) In this study, it was found that the molecules **CQM** and **CQMA** were effective corrosion inhibitors of MS exposed to 1 N HCl solution. The inhibition efficiency increased with an increase in the inhibitors concentration. **CQMA** was found to be the better corrosion inhibitor than **CQM**.
(2) The polarization curves inferred that both **CQM** and **CQMA** have acted as mixed-type inhibitors. The results also demonstrated that the inhibition was attributed to the adsorption of the **CQM** and **CQMA** molecules on the MS surface.
(3) The decrease in the C_{dl} values could be attributed either to the decrease in local dielectric constant and/or an increase in thickness of the **CQM** and **CQMA** through adsorption at the metal–solution interface.
(4) WL, EIS and polarisation techniques yielded consistent results from which inhibition efficiency of **CQMA** was found to be higher than that of **CQM**. Adsorption of **CQM** and **CQMA** under investigation on the MS surface was found to obey the Langmuir adsorption isotherm with standard free energies of adsorption (ΔG^0_{ads}) of -41.66 and -42.53 kJ mol^{-1} respectively.
(5) The results of the WL, electrochemical polarizations and EIS were in good agreement.

Acknowledgments The authors thank Director, S V National Institute of Technology, Surat for encouragement and for providing necessary research facilities.

References

1. D.A. Jones, *Principles and Prevention of Corrosion*, 2nd edn. (Prentice-Hall Inc., Upper Saddle River, 1996)
2. V.S. Sastry, *Corrosion Inhibitors. Principles and Applications* (Wiley, New York, 1998)
3. F. Bentiss, M. Traisnel, M. Lagrenee, J. Appl. Electrochem. **31**, 41 (2001)
4. G. Schmitt, Br. Corros. J. **19**, 165 (1984)
5. S. John, B. Joseph, K.V. Balakrishnan, K.K. Aravindakshan, A. Joseph, Mater. Chem. Phys. **123**, 218 (2010)
6. A.S. Fouda, H.A. Mostafa, H.M. El-Abbasy, J. Appl. Electrochem. **40**, 163 (2010)
7. M.J. Bahrami, S.M.A. Hosseini, P. Pilvar, Corros. Sci. **52**, 2793 (2010)
8. M.A. Quraishi, I. Ahamada, A. Singha, S. Shuklaa, B. Lal, V. Singh, Mater. Chem. Phys. **112**, 1035 (2008)
9. K.M. Govindaraju, D. Gopi, L. Kavitha, J. Appl. Electrochem. **39**, 2345 (2009)
10. R. Solmaza, E. Altunbas, G. Kardas, Mater. Chem. Phys. **125**, 796 (2011)
11. G. Trabanelli, in *Chemical Industries: Corrosion Mechanism*, ed. by F. Mansfeld (Marcel Dekker, New York, 1987), p. 120
12. I.B. Obot, N.O. Obi-Egbedi, Curr. Appl. Phys. **11**, 382 (2011)
13. S. Deng, X. Li, H. Fu, Corros. Sci. **53**, 822 (2011)
14. M.G. Hosseini, H. Khalilpur, S. Ershad, L. Saghatforoush, J. Appl. Electrochem. **40**, 215 (2010)
15. P. Xuehui, R. Xiangbin, K. Fei, X. Jiandong, H. Baorong, Chin. J. Chem. Eng. **18**, 337 (2010)

16. I. Ahamad, C. Gupta, R. Prasad, M.A. Quraishi, J. Appl. Electrochem. **40**, 2171 (2010)
17. M. Lashgaria, M. Arshadib, S. Miandaria, Electrochim. Acta. **55**, 6058 (2010)
18. D. Gopi, K.M. Govindaraju, L. Kavitha, J. Appl. Electrochem. **40**, 1349 (2010)
19. A. Yurt, G. Bereket, A. Kivrak, A. Balaban, B. Erk, J. Appl. Electrochem. **35**, 1025 (2005)
20. S. Bilgice, N. Cealiskan, J. Appl. Electrochem. **31**, 79 (2001)
21. E. Bayol, T. Gurtenb, A.A. Gurtena, M. Erbil, Mater. Chem. Phys. **112**, 624 (2008)
22. G.K. Nagaraja, G.K. Prakash, M.N. Kumaraswamy, V.P. Vaidya, K.M. Mahadevan, ARKIVOC **xv**, 160 (2006)
23. S.D. Srivastava, J.P. Sen, Indian J. Chem. **47B**, 1583 (2008)
24. S.K. Sonwane, S.D. Srivastava, S.K. Srivastava, Indian J. Chem. **47B**, 633 (2008)
25. E. Barsoukov, J.R. Macdonald, *Impedance Spectroscopy; Theory, Experiment, and Applications*, 2nd edn. (Wiley Interscience Publications, Hoboken, 2005)
26. A.J. Bard, L.R. Faulkner, *Electrochemical Methods; Fundamentals and Applications* (Wiley Interscience Publications, New York, 2000)
27. J.R. Scully, D.C. Silverman, M.W. Kendig (eds.), *Electrochemical Impedance: Analysis and Interpretation* (ASTM, West Conshohocken, 1993)
28. F. Mansfeld, Electrochim. Acta. **35**, 1533 (1990)
29. S. Fletcher, J. Electrochem. Soc. **141**, 1823 (1994)
30. S. Zhang, Z. Tao, W. Li, B. Hou, Appl. Surf. Sci. **255**, 6757 (2009)
31. G.E. Badr, Corros. Sci. **51**, 2529 (2009)
32. E. McCafferty, N. Hackerman, J. Electrochem. Soc. **119**, 146 (1972)
33. C. Cao, Corros. Sci. **38**, 2073 (1996)
34. M. Lebrini, M. Lagrenee, H. Vezin, M. Traisnel, F. Bentiss, Corros. Sci. **49**, 2254 (2007)
35. M.El. Azhar, B. Mernari, M. Traisnel, F. Bentiss, M. Lagrenee, Corros. Sci. **43**, 2229 (2001)
36. A. Yurt, A. Balaban, S.U. Kandemir, G. Bereket, B. Erk, Mater. Chem. Phys. **85**, 420 (2004)
37. J.R. Macdonald, W.B. Johnson, in *Theory in Impedance Spectroscopy*, ed. by J.R. Macdonald (Wiley, New York, 1987)
38. O.L. Riggs Jr, in *Corrosion Inhibitors*, ed. by C.C. Nathan (NACE, Houston, 1973), p. 7
39. J. Fu, S. Li, Y. Wang, L. Cao, L. Lu, J. Mater. Sci. **45**, 6255 (2010)
40. S. Martinez, I. Stern, Appl. Surf. Sci. **199**, 83 (2002)
41. T. Szauer, A. Brand, Electrochim. Acta **26**, 1253 (1981)
41. J. Aljourani, K. Raeissi, M.A. Golozar, Corros. Sci. **51**, 1836 (2009)
43. F.M. Donahue, K. Nobe, J. Electrochem. Soc. **112**, 886 (1965)
44. E. Kamis, F. Bellucci, R.M. Latanision, E.S.H. El-Ashry, Corrosion **47**, 677 (1991)
45. B.M. Mistry, N.S. Patel, M.J. Patel, S. Jauhari, Res. Chem. Intermed. **37**, 659 (2011)
46. K. Mallaiyaa, R. Subramaniama, S.S. Srikandana, S. Gowria, N. Rajasekaranb, A. Selvaraj, Electrochim. Acta **56**, 3857 (2011)
47. X. Li, S. Deng, H. Fu, T. Li, Electrochim. Acta **54**, 4089 (2009)
48. T.P. Zhao, G.N. Mu, Corros. Sci. **41**, 1937 (1999)
49. F. Bentiss, M. Lebrini, M. Lagrenee, Corros. Sci. **47**, 2915 (2005)
50. E.A. Noor, A.H. Al-Moubaraki, Mater. Chem. Phys. **110**, 145 (2008)
51. R. Solmaz, G. Kardas, M. Culha, B. Yazici, M. Erbil, Electrochim. Acta **53**, 5941 (2008)
52. X. Li, S. Deng, H. Fu, G. Mu, Corros. Sci. **51**, 620 (2009)
53. F. Xu, J. Duan, S. Zhang, B. Hou, Mater. Lett. **62**, 4072 (2008)
54. Q.B. Zhang, Y.X. Hua, Electrochim. Acta **54**, 1881 (2009)
55. S.A. Abd El-Makoud, Appl. Surf. Sci. **206**, 129 (2003)
56. R. Solmaz, G. Kardas, B. Yazici, M. Erbil, Colloids Surf. A. **312**, 7 (2008)
57. H. Keles, M. Keles, I. Dehri, O. Serindag, Mater. Chem. Phys. **112**, 173 (2008)